ENERGY-SAVING TECHNOLOGIES AND EQUIPMENT

The work examines the heat exchange characteristics of a condenser in which heat removal of the refrigerant condensation occurs due to natural convection and radiation cooling. The heat exchanger is designed to reduce energy costs for the removal of condensation heat. Unlike traditional air cooling condensers, it uses radiation cooling, a method of heat removal based on its transmission in the form of infrared radiation through the planet's atmosphere into the surrounding outer space. A method for calculating the thickness of the radiating plate has been developed. To minimize material consumption and cost, the distance between the tubes is reduced to 40 mm, and the thickness of the aluminum radiating plate is reduced to 0.32 mm. The inner diameter of the coolant channels is 1 mm.

For the experimental study of the condenser, an experimental stand working on R134a refrigerant was developed. Theoretical and experimental studies of heat transfer have been carried out. The heat transfer coefficient of the heat exchanger, reduced to the area of the radiating surface, was from 10.3±1.36 to 18.7±2.47 $W \cdot m^{-2} \cdot °C^{-1}$, when the condensation temperature was 12.8...21.9 °C higher than the temperature of atmospheric air. The operability of the condenser is shown both during the day and at night, in the presence of precipitation in the form of rain and snow, and a high level of cloudiness.

The material capacity and filling of the refrigerant in the condenser are comparable to the characteristics of air-cooled condensers with forced air circulation. At the same time, it does not consume electricity. It can be used in stationary refrigeration systems (in data processing centers, commercial refrigeration equipment, air conditioners) to increase their energy efficiency

Keywords: radiation cooling, refrigerating machine, condenser, natural air circulation, energy efficiency

UDC 621.5.044
DOI: 10.15587/1729-4061.2023.273607

CONDENSATION HEAT REMOVAL DUE TO THE COMBINED IMPACT OF NATURAL CONVECTION AND RADIATIVE COOLING

Alexandr Tsoy
Corresponding author
Doctor of Technical Sciences, Associate Professor*
E-mail: tsoyteniz@bk.ru
Alexandr Granovskiy
Senior Researcher*
Baurzhan Nurakhmetov
Doctor of Technical Sciences First Vice-Rector**
Dmitriy Koretskiy
Junior Researcher*
Diana Tsoy-Davis
PhD
Department of Machines and Devices of Manufacturing Processes**
Nikita Veselskiy
Laboratory Assistant*
*Department of Machines and Apparatus for Production Processes**
**Almaty Technological University
Tole bi str., 100, Almaty, Republic of Kazakhstan, A051012

Received date 06.12.2022
Accepted date 09.02.2023
Published date 28.02.2023

How to Cite: *Tsoy, A., Granovskiy, A., Nurakhmetov, B., Koretskiy, D., Tsoy-Davis, D., Veselskiy, N. (2023). Condensation heat removal due to the combined impact of natural convection and radiative cooling. Eastern-European Journal of Enterprise Technologies, 1 (8 (121)), 6–21. doi: https://doi.org/10.15587/1729-4061.2023.273607*

1. Introduction

Refrigeration systems capable of providing the required temperature of the environment in technological equipment in refrigerating chambers, buildings and facilities are expanding their use in the modern developing world. They are widely used in data processing centers, in the cooling systems of shopping centers (supermarkets) and air conditioning.

Refrigeration systems make a significant contribution to the overall level of electricity consumption. As it is known, available energy resources are limited. However, the number of used refrigeration systems continues to grow steadily. In this regard, the search for ways to increase their energy efficiency is underway.

One of the ways to increase energy efficiency is to reduce the energy consumption of individual components of refrigerating machines. In modern refrigerating machines used at the above-mentioned facilities, air cooling condensers with forced air circulation are most often used to remove heat to the environment. In them, energy is consumed by the electric motors of the fan. The power consumption of electric motors is usually up to 5 % of the amount of heat removed.

Radiation cooling (further RC) is a method of lowering the temperature, based on the removal of heat into the surrounding space in the form of infrared radiation through the planet's atmosphere. Thereby RC, it is possible to increase the intensity of heat exchange, as well as obtain a temperature lower than the air temperature in the surface layer of the atmosphere. In recent decades, the possibility of using RC has been widely studied. At the same time, the main attention was paid to the possibility of direct application of RC for cooling the coolant, which takes heat from the cooled object. This approach to the use of RC has not received practical spread. The main problem of this approach is associated with the use of a coolant with a low temperature, due to which the heat flow from a unit area of the radiating surface decreases, capital costs for the creation of heat exchangers and coolant circulation circuits increase.

The use of RC for the direct removal of condensation heat without an intermediate heat carrier in refrigerating

machines is able to increase the heat flow removed from a unit area of the heat exchange surface without the expenditure of electricity and water. Accordingly, with the use of RC, it is possible to create more effective condensers of refrigerating machines. Therefore, studies devoted to increasing the energy efficiency of capacitors due to the use of the combined effect of natural convection and radiation cooling are considered relevant.

2. Literature review and problem statement

In work [1], as well as in many other studies, the possibility of using RC directly to maintain the temperature of the cooled object was considered. At night, RC was used to lower the temperature of the liquid coolant stored in the cold accumulator. During the day, the coolant from the cold accumulator was used to maintain a comfortable air temperature in the cooled room. It was established that the heat exchanger for transferring heat from the coolant to the environment due to radiation cooling and convection (radiator) on average removed 60.8 W of heat from 1 m^2 of the radiating surface per night. Although systems of this type can be used to maintain a comfortable air temperature, they are characterized by a large material capacity. They require the use of radiators with a large area of the radiating surface. The area of the radiating surface can be more than 50 % of the area of the cooled room. Also, a cold battery is needed to maintain the temperature around the clock. The mass of the coolant in the accumulator is about 50...200 kg per 1 m^2 of the cooled room.

Due to the high cost of the RC system components, various ways of reducing it were considered. Many designs of radiators were developed. For example, radiators made of polymer materials were studied [2]. However, the use of such materials causes a decrease in the efficiency of radiators. Or, in the work [3], the possibility of integrating radiators into the roof of the building was considered to reduce total capital costs.

Various ways of accumulating cold were also proposed. For example, in work [4] it is proposed to place the cold accumulator underground. However, despite all the improvements made, RC systems using cold accumulators remain expensive and require a lot of space for placement.

The possibility of using air as a coolant supplied directly to radiators was also considered [5]. In the second work, air was taken from the environment directly through radiators [6]. However, at the same time, the volume occupied by the refrigeration system increases significantly compared to the system in which a liquid coolant is used.

Another approach to reducing the payback period of RC systems is related to increasing the duration of their use during the year. In [7], a study of the possibility of using RC to maintain a low temperature in refrigerating chambers in the conditions of a harsh continental climate during the year was carried out. However, at low temperatures of the atmospheric air, the heat flow removed from the unit area of the radiating surface of the radiator is significantly reduced [8]. There are also problems with cleaning the radiating surface from snow.

In most cases, it is impossible to maintain the required temperature throughout the year only due to RC. Therefore, RC is used together with other methods of cooling (with refrigerating machines, evaporative cooling, etc.). For example, the joint use of RC and a steam-compressor refrigerating machine is studied in [7]. However, the combination of various cooling methods increases capital costs for the creation of a cooling system.

In works [9, 10], a variant of using RC for removal of condensation heat and supercooling of the refrigerant in a vapor-compressor refrigerating machine is proposed. In the proposed system, the heat of condensation is transferred to the liquid coolant, and the liquid coolant is cooled in the radiator. In this case, the radiator has a special coating on the radiating surface, which has a selective spectrum of radiation and absorption (hereinafter «selective coating»). Due to this, the radiator can cool the coolant below the ambient temperature even during the day. In this case, the coolant temperature should be lower than the condensation temperature. The temperature of the coolant entering the radiators was approximately 5 °C higher than the ambient temperature. At the same time, theoretically due to radiation and convection, up to 100 W of heat was removed from 1 m^2 of the radiating surface. In the study, the radiator was also made in such a way that convective heat exchange with the environment was limited. In conditions when the temperature of the radiator is higher than the ambient temperature, there is no need to take measures to reduce convective heat exchange, as this reduces the total heat flow.

The solution with the supply of an intermediate liquid coolant in the radiator in the listed works is usually associated with a decrease in the operating pressure in the radiator. But it has the following disadvantages:

1. Energy is spent on the circulation of the coolant.

2. The coolant must have a temperature lower than the temperature of the cooled object.

To increase the heat flow from the radiating surface:

1. It will increase the temperature of the radiating surface, since according to the Stefan-Boltzmann law, the amount of radiated heat is proportional to the fourth degree of temperature.

2. Exclude intermediate circuits for the coolant.

To exclude intermediate coolant circuits, a refrigeration system was previously proposed, in which cooling occurs due to the natural circulation of the coolant through the radiators [11]. The study showed that such a system can work without consuming electricity. However, due to the low coefficient of heat transfer from the coolant to the radiating surface, as well as the low temperature of the radiating surface, the radiator dissipated no more than 13.9 W/m^2. It was also necessary to fill the radiator with a relatively large amount of coolant.

In work [12] a method of cooling is proposed, in which RC and convection are used to remove heat coming through heat tubes. The presented structure dissipated no more than 15...20 W/m^2 on average per night. The use of a microchannel heat tube and an increase in the temperature of the cooled medium above the air temperature by 10 °C in work [13] led to an increase in the theoretical heat flux from the radiating surface to 250 W/m^2. But the proposed cooling scheme can work only if the temperature of the cooled object is significantly higher than the temperature of the atmospheric air. Accordingly, changes in the temperature of the environment can in this case affect the temperature of the cooled object, which in some cases is undesirable. Also, in this work, the design parameters of the heat tube used to transport the coolant to the radiating surface are studied in detail. But the structural parameters of the radiating surface of the radiator were not investigated.

Traditional condensers of air cooling of finned-tube design are not designed to remove heat in the form of radiation. To increase their efficiency, work was carried out aimed at increasing the coefficients of heat transfer from the refrigerant to the tubes and from the fins to the air flow. These works led to the creation of minichannel (or microchannel) heat

exchangers [14]. In such heat exchangers, the heat transfer coefficient reaches 60 W/(m^2·K), which allows reducing their size [15]. But for this, as in finned-tube condensers, a forced supply of air is required due to the consumption of electricity. Reducing the size of the channels in such heat exchangers leads to increased aerodynamic resistance and increased consumption of electricity by the fan motor. Also, their use allows in some cases to reduce the required refueling of the refrigerant [16].

Taking into account the listed circumstances, in this work it is proposed to abandon the use of an intermediate coolant and schemes with natural circulation of the refrigerant, and to directly feed the refrigerant pumped by the compressor into the heat exchanger. Thus, it is proposed to create a mini-channel condenser (hereinafter MC), in which the removal of the heat of condensation of the refrigerant is carried out due to the joint effect of natural convection of air and RC. This approach has not been studied before. Accordingly, it is not known whether the technical characteristics of such a heat exchanger can be compared with heat exchangers of traditional designs. The main disadvantage of the proposed solution is the large overall dimensions of the resulting heat exchanger, since in this case it is impossible to lay a multilayer heat exchange surface, as is done in finned tube heat exchangers. Also, the increase in overall dimensions may be due to increased filling of the refrigerant. It is also unknown how the parameters of the environment will affect its work. In particular, it is important to understand whether it will be able to remove heat not only at night, but also during the day, and whether atmospheric precipitation in the form of rain and snow will affect it.

3. The aim and objectives of research

The aim of the study is to identify the features of the condensation heat removal process under the combined effect of natural air convection and radiation cooling, in which a mini-channel condenser was created to increase the efficiency of heat transfer to the environment.

To achieve the aim, the following objectives are set:

– on the basis of a theoretical study of heat exchange processes, determine the main geometric design dimensions of the minichannel condenser and carry out their optimization to minimize the cost of the design;

– experimentally investigate the heat transfer coefficient of the minichannel condenser under changing environmental conditions;

– will compare the characteristics of the minichannel condenser with the characteristics of already existing condensers of air cooling.

4. Methods of research

4. 1. Design of a minichannel capacitor

To condense the refrigerant, it is suggested to use the MC design shown in Fig. 1. It represents a set of parallel copper capillary tubes 2, attached to a thin aluminum sheet 4. The capillary tubes are soldered to the distribution and collecting collectors (1 and 2).

The refrigerant enters the distribution manifold 1. Then it is distributed through capillary tubes, where it cools and condenses. The liquid refrigerant flows into the collector 3.

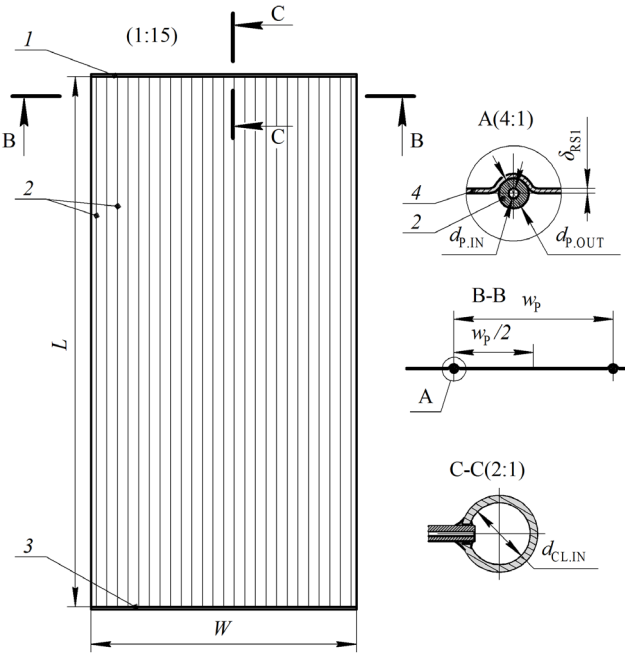

Fig. 1. MC design: 1 – distribution manifold; 2 – capillary tubes; 3 – collecting collector; 4 – radiating plate

The method of attaching the radiating plate to the capillary tubes is shown in Fig. 2. The loops have a width of 5 mm and are made with a pitch of 80 mm.

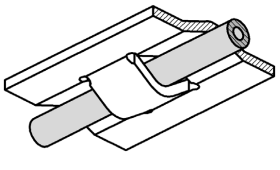

Fig. 2. Method of fastening the capillary tube

There is no thermal insulation in this MC. Also, there is no transparent screen above the emitting surface. Due to these solutions, the convective removal of heat to the environment increases and the material capacity of the structure decreases.

Theoretical methods for calculating the geometric characteristics of the radiator for given conditions of application are presented below.

4. 2. Theoretical methods used to calculate the minichannel capacitor

4. 2. 1. Calculation of the heat flux removed from the radiating surface of the minichannel capacitor

The emitting plate MC is a flat metal sheet. Its upper radiating surface transmits heat to the environment due to natural convection and radiation, and the lower surface transmits heat only due to convection. The heat flux from the radiating plate, the length and width of which is 1 m, will be (W/m^2):

$$q_{SUM} = q_{CONV.UP} + q_{CONV.DOWN} + q_{RAD}, \quad (1)$$

where $q_{CONV.UP}$ – the convective thermal flux from the upper side of the radiating plate facing the sky, W/m^2; q_{RAD} – the heat flux from the upper side of the radiating plate due to radiation, W/m^2; $q_{CONV.DOWN}$ – convective flow from the lower side of the radiating plate, W/m^2.

When calculating, let's consider that the entire radiating plate has the same temperature.

The heat flow, removed due to radiation at night from a surface with a normal radiation/absorption spectrum, is calculated according to the well-known formula (W/m^2):

$$q_{RAD} = \sigma \cdot \varepsilon_{RAD} \cdot \left[\left(t_{RAD} + 273.15 \right)^4 - T_{SKY}^4 \right], \quad (2)$$

where σ – the Stefan-Boltzmann constant, $5.67 \cdot 10^{-8}$ W·m^{-2}·K^{-4}; ε_{RAD} – the relative emissivity of the surface. In the calculations, let's assume that $\varepsilon_{RAD}=0.9$; t_{RAD} – the temperature of the radiating surface, °C; T_{SKY} – conditional (imaginary) sky temperature, K.

The conditional temperature of the night sky is calculated according to the formula [17]:

$$T_{SKY} = \left(t_{AIR} + 273.15 \right) \cdot \left(\varepsilon_{SKY} + CF_{AL} \right)^{0.25} \cdot CF_{CL}^{0.25}, \quad (3)$$

where t_{AIR} – the temperature of atmospheric air in the surface layer, °C; ε_{SKY} – the emissivity of the sky; CF_{AL} – the coefficient that takes into account the influence of atmospheric pressure; CF_{CL} – the coefficient that takes into account the influence of cloudiness.

The emissivity of the sky is calculated by the expression:

$$\varepsilon_{SKY} = 0.787 + 0.764 \cdot \ln\left(\frac{t_{DEW} + 273.15}{273} \right), \quad (4)$$

where t_{DEW} – the dew point temperature of the air in the surface layer, °C.

The correction taking into account the influence of atmospheric pressure CF_{AL} and the correction taking into account the influence of cloud cover CF_{CL} are calculated according to the formulas from work [18].

For a radiating surface with a special optical coating with a selective emission/absorption spectrum, the heat flow removed due to radiation during the day can be simplified by the expression from work [19] based on data [20].

The heat flow removed due to convection q_{CONV} from the upper and lower sides of the radiating plate is calculated according to the standard method according to the heat transfer coefficient α for natural air convection. At the same time, the Nusselt number is determined by the formula [21]:

$$Nu_{FC} = m \cdot d \cdot \left(\mathrm{Gr} \cdot \mathrm{Pr} \right)^n, \quad (5)$$

where Gr – the Grashof number; Pr – Prandtl number; m, n – the coefficients determined depending on the value of the product Gr·Pr according to the table 1; d – the coefficient determined depending on the location of the surface in space, as well as whether the surface temperature is higher than the air temperature. For the case of a surface oriented upwards, when its temperature is higher than the air temperature, the coefficient $d=1.3$. For a surface oriented downward, when its surface temperature is higher than air temperature $d=0.7$.

Table 1

Values of coefficients for calculating the Nusselt number

Gr·Pr	m	n
(0.001; 500]	1.18	1/8
(500; $2 \cdot 10^7$]	0.54	1/4
($2 \cdot 10^7$; $1 \cdot 10^{13}$]	0.135	1/3

The total coefficient of heat transfer of the radiating plate, reduced to the area of the upper radiating surface (W·m^{-2}·°C^{-1}):

$$\alpha_{SUM} = \left| \frac{q_{CONV.UP} + q_{CONV.DOWN} + q_{RAD}}{t_C - t_{AIR}} \right| = \left| \frac{q_{SUM}}{\Delta t_{MC}} \right|, \quad (6)$$

where Δt_{MC} – the temperature pressure on the minichannel condenser, defined as the difference between the condensation temperature of the refrigerant vapor t_C in MC and the temperature of the atmospheric air t_{AIR}, °C.

4. 2. 2. Required diameter of refrigerant tubes

The required diameter of the round tube of the minichannel capacitor (m):

$$d_{P.IN} = \sqrt{\frac{4}{\pi} \cdot \frac{\vartheta}{\upsilon_L} \cdot \left(\frac{0.001 \cdot q_{SUM} L_P \varpi_P}{i_2' - i_3} \right)}, \quad (7)$$

where ϑ – the specific volume of refrigerant, m^3/kg; υ_L – the optimal speed of movement of the liquid coolant leaving the tube, m/s. In this case, its value is 0.5 m/s; L_P – tube length, m; i_2' and i_3 – the enthalpy of the refrigerant at the inlet and outlet of the minichannel condenser, kJ/kg.

4. 2. 3. Heat transfer coefficient from the condensing refrigerant of the tube wall

The average value of the Nusselt number for the condensing refrigerant vapor inside the tubes is calculated using the formula for the case of condensation of the moving steam flow inside the tube during turbulent condensate flow. At the same time, if the diameter of the coolant tube is in the range from 0.31 to 3.30 mm, the formula from work [22] is used.

Taking into account the limitations of the method under consideration, the initial degree of dryness of the refrigerant is $x_1=0.9$, and the final degree of dryness is $x_2=0.1$. Then,

$$\overline{Nu}_R = 29.486 \, \mathrm{Re}_L^{0.258} \, \mathrm{Pr}_L^{-0.495} \, \pi_{CR}^{-0.288}, \quad (8)$$

where Re_L – the Reynolds number for the liquid refrigerant at the outlet of the refrigerant condensation section; Pr_L – the Prandtl number for the liquid refrigerant at the outlet of the refrigerant condensation section; π_{CR} – the ratio of the saturated vapor pressure of the refrigerant p_S to the critical pressure of this refrigerant p_{CR}, calculated as $\pi_{CR}=p_S/p_{CR}$.

For channels with an inner diameter of more than 3.3 mm, it is permissible to use the formula from work [23].

The average heat transfer coefficient from the refrigerant to the tube wall:

$$\overline{\alpha}_R = \overline{\mathrm{Nu}}_R \cdot \frac{\lambda_L}{d_{P.IN}}, \quad (9)$$

where λ_L – the thermal conductivity of the liquid refrigerant, W·m^{-1}·°C^{-1}; d_{IN} – the internal diameter of the refrigerant pipeline, m.

4. 2. 4. Determination of the permissible temperature change along the length of the radiating surface

The emitting surface of the minichannel capacitor in the space between the tubes will have a lower temperature than the temperature of the surface directly above the capillary tubes. A decrease in the temperature of the radiating surface in the intertube space leads to the fact that less heat is released from the radiating surface into the environment.

The amount of heat that is removed from the radiating surface of the radiator can be simplified as:

$$q_{SUM} = \alpha_{SUM} \Delta t_{MC}. \quad (10)$$

If the total heat transfer coefficient α_{SUM} is considered constant, then the heat flow depends only on the temperature pressure Δt_{MC}. Let the temperature of the radiating surface in the intertube space vary linearly. Then directly above the tube it will have a temperature of t_{PL1}, and in the center between the tubes t_{PL2}. Let $t_{PL2}=t_{PL1}-\Delta t_{PL}$, where Δt_{PL} – the change in temperature along the length of the radiating surface. Then, the average temperature pressure between the radiating surface and the air:

$$\overline{\Delta t}_{MC} = \left(t_{PL1} - t_{AIR}\right) - \frac{\Delta t_{PL}}{2}. \quad (11)$$

The efficiency coefficient of heat transfer from the radiating surface MC is determined by the expression:

$$\eta_{MC} = \frac{\overline{\Delta t}_{MC}}{\overline{\Delta t}_{MC.N}}, \quad (12)$$

where $\overline{\Delta t}_{MC.N}$ – the average temperature pressure on the radiating surface, determined under the condition that the entire radiating surface has the same temperature.

Substituted expression (11) into formula (12), and also assumed that $\left(t_{PL1} - t_{AIR}\right) \approx \overline{\Delta t}_{MC.N}$, the permissible temperature change along the length of the radiating surface:

$$\Delta t_{PL} = 2 \cdot \overline{\Delta t}_{MC.N} \cdot \left(1 - \eta_{MC}\right). \quad (13)$$

4. 2. 5. Calculation of the thickness of the radiating plate

The emitting surface should have approximately the same temperature at all points. To determine the minimum thickness of the radiating plate, at which this condition is fulfilled, the heat flow passing through it was considered (Fig. 3).

The amount of heat that passes from the tube through section A due to thermal conductivity must be equal to the amount of heat that passes through part of the radiating surface of the plate located to the right of section A. Therefore, with a linear temperature change along x, the thickness of the radiating plate Δ_{PL} in section A (m):

$$\delta_{PL} = \frac{q_{SUM} \cdot x_A \cdot \left(0.5 w_P - x_A\right)}{\Delta t_A \cdot \lambda_{PL}} = \frac{q_{SUM} \cdot w_P \cdot \left(0.5 w_P - x_A\right)}{2 \Delta t_{PL} \cdot \lambda_{PL}}, \quad (14)$$

where x_A – the distance from the left edge of the plate to the section under consideration, m; λ_{PL} – thermal conductivity coefficient of the plate material, $W \cdot m^{-1} \cdot °C^{-1}$; Δ_{PL} – the plate thickness in section A, m; where Δt_A – the temperature change between the left edge of the radiating plate and section A.

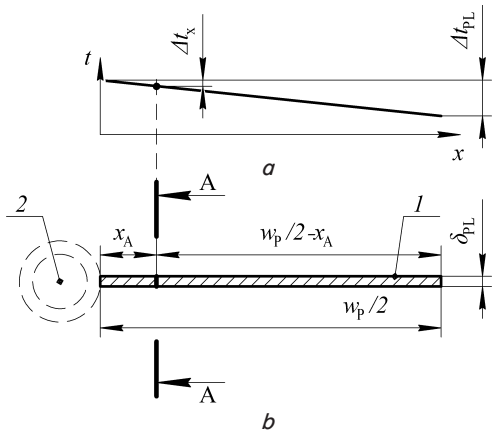

Fig. 3. Scheme for calculating the heat flow through the radiating plate: *a* – graph of temperature change along the length of the radiating plate; *b* – dimensions of the radiating plate; 1 – radiating plate; 2 – capillary tube

After taking $x_A=0$, the formula for calculating the required thickness of the radiating plate near the capillary tube (m) is obtained:

$$\delta_{PL} = \frac{q_{SUM}}{\Delta t_{PL}} \cdot \frac{w_P^2}{4 \lambda_{PL}}. \quad (15)$$

4. 2. 6. Calculation of the wrap angle of the tube

The amount of heat that passes through the contact surface of the tube and the radiating plate must be equal to the amount of heat transferred from the radiating surface to the environment. The thermal resistance of the tube wall and the gap between the contact surfaces must be low enough so that the temperature of the radiating plate does not fall significantly below the coolant temperature.

The amount of heat transferred from one tube, 1 m long, to the radiating surface (W) through the contact surface C is determined by the thermal resistance of the tube wall R_P and the thermal resistance of the gap R_C (Fig. 4). In this case, the thermal resistance of the gap depends on the contact area FC between the tube and the radiating plate.

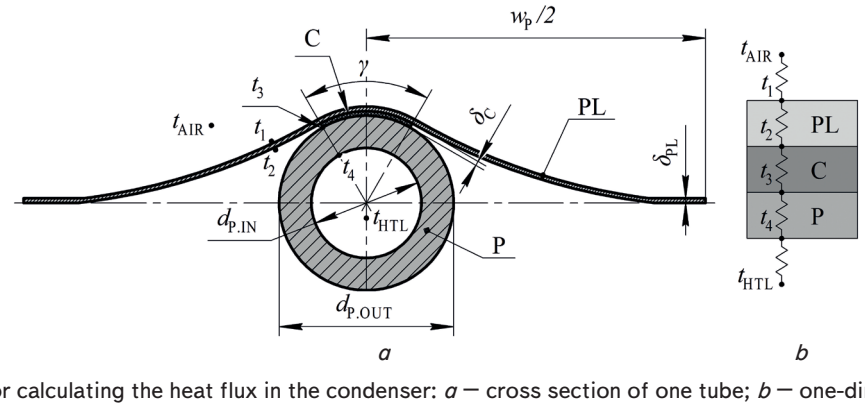

Fig. 4. Scheme for calculating the heat flux in the condenser: *a* – cross section of one tube; *b* – one-dimensional scheme for calculating the heat transfer coefficient; PL – radiating plate; P – tube for refrigerant; C – gap filler

Therefore, the minimum angle of coverage of the tube by the radiating surface γ_{MIN} (°) for the transmission of a given amount of heat q_{SUM} with a known allowable temperature change Δt_2:

$$\gamma_{MIN} = \frac{360 \cdot w_P \cdot q_{SUM} \cdot \lambda_P \cdot (\Delta_P + \Delta_{PL})}{d_{P.OUT} \cdot \lambda_C \cdot \left[2\pi \cdot \lambda_P \cdot \Delta t_2 - w_P \cdot q_{SUM} \cdot \ln\left(\frac{d_{P.OUT}}{d_{P.IN}} \right) \right]}, \quad (16)$$

where Δ_C – the average gap between the contact surfaces, m; λ_C – thermal conductivity of the material filling the gap, W·m^{-1}·°C^{-1}; λ_P – thermal conductivity of the tube material, W·m^{-1}·°C^{-1}; Δ_P – copper tube surface roughness, 2·10^{-6} m; Δ_{PL} – surface roughness of aluminum sheet, 6·10^{-5} m; Δt_2 – allowable temperature change between the inner surface of the tube, washed by the refrigerant, and the surface of the radiating plate above the tube, °C; $d_{P.OUT}$ and $d_{P.IN}$ – the outer and inner diameters of the tube, m.

4. 2. 7. Heat transfer coefficient of minichannel condenser

The calculation of the heat transfer coefficient was carried out on the basis of the methodology proposed in [24]. Consideration of the heat flow transmitted from the refrigerant condensing in one tube to the environment showed the following (Fig. 4). The heat flux transferred from the refrigerant to the tube wall is equal to the amount of heat passing through all elements of the minichannel condenser and is equal to the heat flux removed from the radiating surface. Then the heat flux transmitted from the radiating plate with a length and width of 1 m (W/m^2):

$$q_{SUM} = \frac{k_P}{w_P} \cdot (t_{HTL} - t_{AIR}) = k_{MC} \cdot \Delta t_{MC}, \quad (17)$$

where $k_{MC}=k_P/w_P$ – the heat transfer coefficient of the minichannel condenser, reduced to the area of the radiating surface, W·m^{-2}·°C^{-1}; t_{HTL} – the temperature of the substance fed into the tube, °C.

In the formula above, the heat transfer coefficient of the tube is calculated as:

$$k_P = \frac{1}{\left[\frac{1}{\alpha_{SUM} \cdot w_P} + \frac{1}{k_{PL} \cdot w_P} + \frac{1}{k_C \cdot F_C} + \frac{1}{k_{WP}} + \frac{1}{\alpha_R \cdot F_{P.IN}} \right]}. \quad (18)$$

Here,

$$F_{P.IN} = \pi \cdot d_{P.IN}; \quad (19)$$

$$k_{WP} = \frac{2\pi\lambda_P}{\ln\left(\frac{d_{P.OUT}}{d_{P.IN}} \right)}; \quad (20)$$

$$k_C = \frac{\lambda_C}{\delta_C}; \quad (21)$$

$$k_{PL} = \frac{\lambda_{PL}}{\delta_{PL}}; \quad (22)$$

$$F_C = \frac{\gamma}{360} \cdot \pi \cdot d_{P.OUT}, \quad (23)$$

where γ – the angle of coverage of the tube by the radiating surface.

4. 2. 8. Calculation of material consumption and cost of materials of a minichannel condenser

Mass of 1 m^2 of radiant plate without refrigerant charge:

$$m_{MC} = m_P + m_{PL} + m_{THP}, \quad (24)$$

where m_P – the mass of MC tubes per 1 m^2 of radiating surface, kg/m^2; m_{PL} – the mass of the MC radiating plate, kg/m^2; m_{THP} – the mass of thermal paste, kg/m^2.

Mass of thermal paste (kg/m^2):

$$m_{THP} = \frac{(\Delta_P + \Delta_{PL})}{2} \cdot \frac{\gamma}{360} \cdot \pi \cdot d_{P.OUT} \cdot \frac{W}{w_P} \cdot \rho_{THP}, \quad (25)$$

where ρ_{THP} – the thermal paste density, kg/m^3; W – MC width, m. The cost of materials for 1 m^2 of minichannel condenser (USD/m^2):

$$CS_{MC} = CS_{PL} + CS_P \cdot \frac{1}{w_P} + CS_{THP} + CS_{SC}, \quad (26)$$

where CS_{PL} – the cost of the radiating plate, USD/m^2; USD; CS_P – the cost of tubes, USD; CS_{THP} – the cost of thermal paste, USD/m^2; CS_{SC} – the cost of selective coating of the radiating surface of a minichannel capacitor, USD/m^2.

The cost of 1 m^2 of the radiating plate of the CS_{PL} minichannel capacitor and the cost of the CS_{THP} thermal paste are calculated based on their mass.

For tubes, their cost linearly depends on the diameter. So, taking into account the retail prices available in the city of Almaty, the cost of 1 m of copper capillary tube is determined by the expression (USD/m):

$$CS_P = 404.8 \cdot d_{P.IN} + 0.35, \quad (27)$$

where $d_{P.IN}$ – the inner diameter of the capillary tube, m.

4. 2. 9. Amount of refrigerant in the mini-channel condenser

Refrigerant mass in MC (kg):

$$m_R = \frac{\pi W}{4} \cdot (\rho_L + \rho_V) \cdot \left(\frac{0.5 \cdot L}{w_P} d_{P.IN}^2 + d_{CL.IN}^2 \right), \quad (28)$$

where ρ_L – the density of the liquid refrigerant at pressure in the MC, kg/m^3; ρ_V – the density of the vaporous refrigerant at pressure in the MC, kg/m^3; $d_{P.IN}$ – the internal diameter of capillary tubes for refrigerant, m; $d_{CL.IN}$ – the internal diameter of the distribution and collection manifold for the refrigerant, m.

4. 3. Method of experimental study of heat transfer in a minichannel condenser

4. 3. 1. Design of the experimental stand

To study the characteristics of MC, an experimental stand was developed (Fig. 5). It is a conventional single-stage vapor compressor refrigeration machine. However, it uses an MC as a heat exchanger to condense the refrigerant.

The evaporator is a heat exchanger made of two coaxial copper tubes 3/8» (9.52 mm) and 1/2» (12.5 mm). The refrigerant is supplied to the annular space. The length of the tubes is 800 mm. Outside, the evaporator is thermally insulated with 18 mm thick rubber foam. A TEH tubular resistance heater is inserted into the inner tube of the evaporator. It creates a thermal load. Electrical resistance TEH is 24.6±0.5 ohm at +20 °C. The TEH diameter is 8.5 mm. Its rated power is 400 watts.

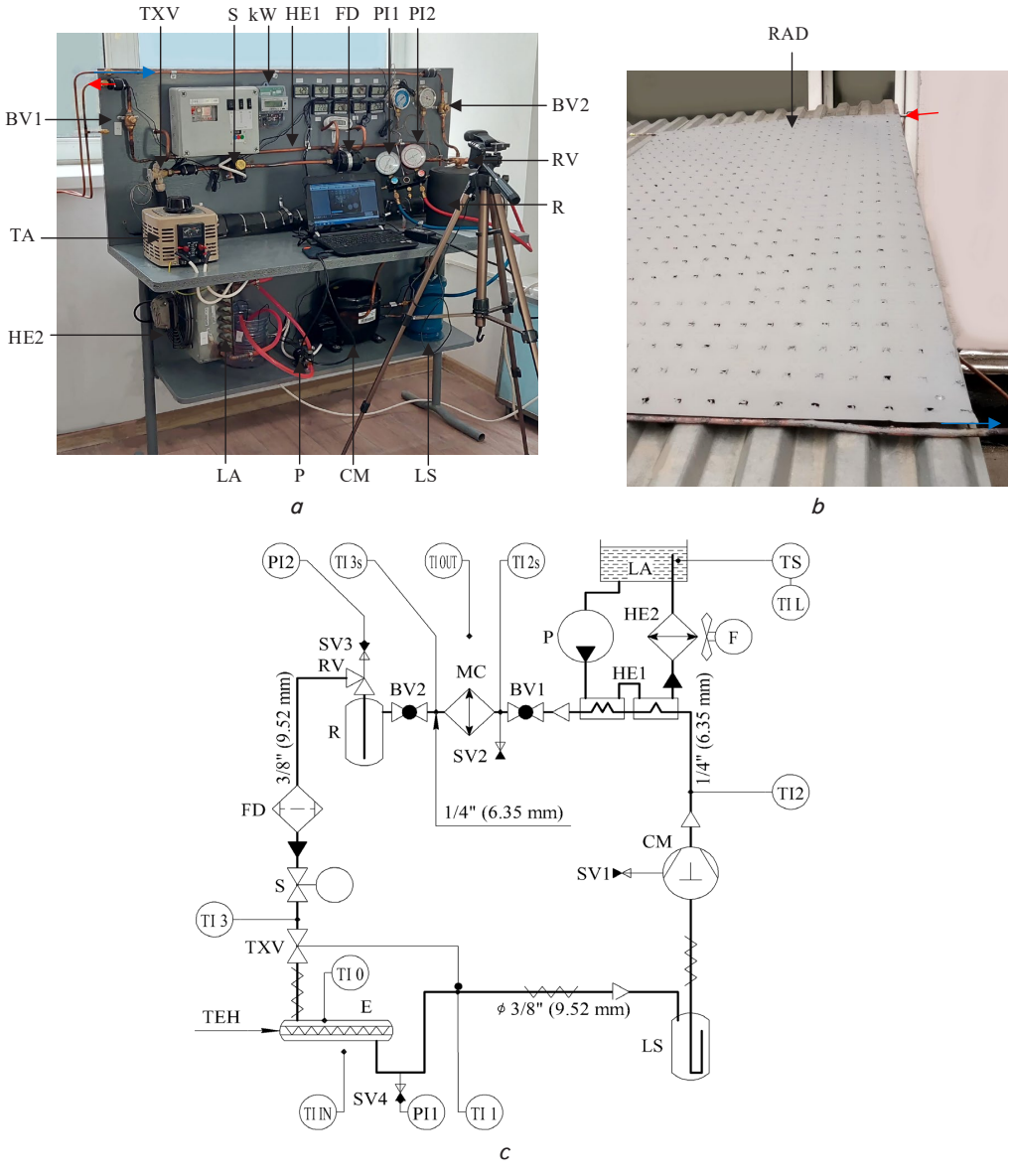

Fig. 5. Experimental stand: *a* — appearance; *b* — appearance of the minichannel capacitor; *c* — hydraulic diagram with temperature sensor placement points; BV1, BV2 — ball valves; CM — compressor; E — evaporator; F — fan; FD — filter-drier; HE1 — liquid cooling heat exchanger; HE2 — air cooled heat exchanger; kW — electric meter; LA — liquid accumulator; LS — liquid separator; MC — minichannel capacitor; P — pump; PI — manometer; R — receiver; RV — Rotalok vlve; S — solenoid valve; SV1...SV4 — service fittings; TA — laboratory autotransformer; TEH — tubular electric heater; TI — thermometers; TS — thermostat; TXV — thermal expansion valve

The power of TEH is regulated by changing the supply voltage. For this, a laboratory autotransformer Matrix TDGC-1 (China) is used. The power consumed by TEH is measured at the input of a laboratory autotransformer using an Orman SOAP-E717-TX electricity meter (Kazakhstan). Active power measurement accuracy class – 1 according to GOST R 52322-2005. Relative error when measuring power consumption <5 %. Measurement error ±5 W. Let's neglect power losses in the laboratory autotransformer.

The experimental bench uses a hermetic piston compressor Embraco EG130HLR (Brazil). The piston volume is 10.61 cm^3. According to the manufacturer, the compressor has a cooling capacity of 343 W at a condensing temperature of +35 °C and an evaporating temperature of –20 °C (Test Condition: EN12900LBP, Return Gas 20 °C, Subcooling 0 °C). Lubricant POE ISO22, 230 ml.

To regulate the supply of refrigerant to the evaporator, a mechanical expansion valve TXV Danfoss T2 (Denmark), (code 068Z3346) with valve assembly No. 00 (code 068-2003) is used.

When the supply voltage is increased, the TEH TXV increases the refrigerant flow to the evaporator. In this way, the cooling capacity and the heat output transmitted to the MC are regulated.

When pump P is turned on, heat exchanger HE1 cools the superheated refrigerant vapor leaving compressor CM. By switching on/off the fan F while the pump P is on, the temperature of the water, and therefore the temperature of the refrigerant entering the radiator, is controlled.

The HE1 heat exchanger is a tube-in-tube design made of copper tubes with countercurrent flow. The refrigerant is supplied to the inner tube, and the water to the annulus.

The inner tube diameter is 1/4» (6.35 mm) and the outer tube is 3/8» (9.52 mm). The heat exchanger consists of two consecutive sections. The first section has a length of 576 mm, and the second 286 mm. The area of the heat exchange surface of the 1st section is 0.0115 m^2, and the 2nd section is 0.0057 m^2. The total area of the heat exchange surface is 0.0172 m^2. Water is supplied to this heat exchanger by a pump P from a liquid accumulator LA. The volume of water in the liquid accumulator LA and all piping is 3 liters. The used pump DC40E-1250 (China) with a power of 13.2 W, a maximum coolant flow rate of 8.3 l/min and a head of 5 m. surface 1.53 m^2.

An LS liquid separator is installed at the compressor inlet to protect the compressor from liquid refrigerant. Model of liquid separator is GVN SLA 5/8 (Turkey).

A container with an internal volume of 2.5 liters is used as a linear receiver. The filter drier Blue BLR/EK-053 (China) is installed at the outlet of the receiver. The solenoid valve Castel SV-1068/4 (Italy) is also installed on the liquid pipeline. The experimental bench is charged with Sanmei R134a refrigerant (China).

The experimental stand used a microchannel capacitor, the design of which is shown in Fig. 1. At the same time, its design parameters are as follows. The inner diameter $d_{P.IN}$ of the capillary tubes is 1 mm. Pitch between tubes ϖ_P=40 mm. The suction and distribution manifolds are made of 3/8″ (9.52 mm) copper tube. The length of the radiating surface is 2 m, the width is 1 m. The thickness of the radiating plate is Δ_{PL1}=0.8 mm.

The radiating surface is painted with gray glyptal primer GF-21 to increase the relative emissivity.

The experimental stand is designed to operate at the boiling temperature t_0=−25...−10 °C; condensing temperatures t_c=+20...+50 °C; when changing the cooling capacity from 70 to 400 W. In this case, the generated thermal load on the MC can be from 50 to 250 W/m^2.

Dallas Instruments DS18B20 sensors (China) with an error of ±0.5 °C (within −10...+85 °C) were used for temperature measurement. Boiling pressure (PI1) was measured using a P&M 68 mechanical pressure gauge (China), measuring range −1...+15 bar, error ±0.1 bar. To measure the condensation pressure (PI2), a mechanical pressure gauge P&M 68 (China) was used, measuring range 0...+34 bar, error ±0.2 bar.

To measure the voltage in the external power supply, as well as to measure the power supply voltage TEH at the output of the autotransformer, a UNI-T UT50C voltmeter was used, the measurement range was 0...750 V, the error was ±5.5 V.

The experimental stand is placed inside a heated room. The MC is located outdoors on the north side of the building in such a way that sunlight does not hit the radiating surface. The radiating surface MC is oriented in the north direction and has a slope of 10° to the horizontal plane. The MC is attached to a profiled sheet canopy 1 m above the ground.

The experimental stand is located in Almaty, Republic of Kazakhstan (43°15′N, 76°51′E).

4. 3. 2. Determination of the heat transfer coefficient

To calculate the heat flux transferred to the MC and its heat transfer coefficient based on the data obtained from the experimental bench, the following method was used.

The boiling point of the refrigerant $_{t0}$ is determined by the pressure gauge PI1 on the basis of reference data on the saturated vapors of the refrigerant. The condensing temperature t_C is determined from the PI2 pressure gauge:

$$t_0 = f(p_0), \tag{29}$$

$$t_C = f(p_C). \tag{30}$$

The thermodynamic properties of the refrigerant were calculated using the CoolProp 6.1 module [25] for Microsoft Excel running in the Microsoft Windows 7 operating system.

The thermal power released by TEH is determined directly from the readings of the wattmeter built into the kW meter, as well as from the formula:

$$Q_{TEH} = \frac{U_{TEH}^2}{R_{TEH}}, \tag{31}$$

where U_{TEH} – TEH, supply voltages V; R_{TEH} – TEH electrical resistance, Ohm.

Heat gain to the refrigerant in the evaporator from atmospheric air through thermal insulation (W):

$$Q_E = k_E(t_{IN} - t_0), \tag{32}$$

where k_E – the heat transfer coefficient of the heat-insulating casing of the evaporator, W/m2. For the existing evaporator design, its value does not exceed 0.32 W·°C^{-1}; t_{IN} – the air temperature in the room where the experimental stand is located, °C; t_0 – the boiling point of the refrigerant in the evaporator, °C.

Cooling capacity (W):

$$Q_0 = Q_{TEH} + Q_E. \tag{33}$$

The relative error in determining the cooling capacity under given conditions using the indicated measuring instruments does not exceed 2.2 %.

The refrigerant inlet i_3 (kJ) and outlet i_1 (kJ) enthalpies of the evaporator are determined based on evaporating pressure, condensing pressure, TI3 and TI1 thermometer temperatures:

$$i_1 = f(t_1, p_0), \tag{34}$$

$$i_4 = f(t_3, p_C). \tag{35}$$

Mass flow of refrigerant (kg/s):

$$G_R = \frac{0.001 \cdot Q_0}{i_1 - i_4}. \tag{36}$$

Refrigerant enthalpy at the inlet and outlet of the radiator (kJ/kg):

$$i_{2S} = f(t_{2S}, p_C), \tag{37}$$

$$i_{3S} = f(t_{3S}, p_C). \tag{38}$$

Thermal power dissipated by MC (W):

$$Q_{MC} = 1{,}000 \cdot (i_{2S} - i_{3S}) \cdot G_R. \tag{39}$$

The relative error in determining the thermal power does not exceed 3.4 % when using the measuring instruments indicated above.

The heat transfer coefficient of the radiator, referred to the area of the radiating surface (W·°C^{-1}·m^2):

$$k_{MC}=\frac{Q_{MC}}{A_{MC}\left(t_C-t_{OUT}\right)}, \quad (40)$$

where t_{OUT} – the atmospheric air temperature in the surface layer, °C.

The relative error in determining the heat transfer coefficient by the given method is no more than 13.2 %.

The sequence of measurements is as follows. Compressor CM and heater TEH were switched on at the set time. Also, in some experiments, pump P was turned on. Then the compressor worked for 15 minutes until all parameters of the refrigeration cycle stabilized. Temperatures and pressures were recorded for 45 minutes. For each moment of time, the parameters were calculated using formulas (29)–(40). Next, the values of each parameter were averaged over a specified time interval.

5. Results of experimental and theoretical studies of heat transfer processes in a minichannel condenser

5. 1. Calculation of the design parameters of a minichannel capacitor

5. 1. 1. Heat transfer from the surface of a minichannel condenser

The calculation of the total heat transfer coefficient from the MC radiating plate according to (6) was carried out. It is assumed in the calculations that the temperature of the atmospheric air is in the range from +5 to +35 °C, there is no cloudiness, there is no wind, the relative humidity of the air is 40 %, the MC is located at sea level (atmospheric pressure is 1 Bar). Since the MC may differ in the type of coating of the radiating plate, it may work in the daytime or at night, and it may also be thermally insulated from below, the calculations were carried out for different scenarios presented in Table 2. In all scenarios, it was assumed that the MC was not exposed to direct sunlight.

From Fig. 6, *a*, it can be seen that an increase in the temperature difference t_{MC} leads to an increase in the heat flux from 1 m^2 of the radiating plate. At a temperature difference t_{MC} of 15 °C, without taking into account radiation from the upper and lower sides, a maximum of q_{SUM0}=126 W/m^2 was assigned; during heat exchange due to radiation and convection, q_{SUM1}=224 W/m^2 was removed only from the upper side of the radiating plate; during heat exchange due to radiation and convection, q_{SUM2}=268.4 W/m^2 was removed from the upper and lower sides of the radiating plate. From this it is possible to conclude that radiative cooling in a given temperature regime makes a significant contribution to the amount of heat removed.

It is also worth noting that the use of the lower surface of the radiating plate increases the heat flux by no more than 19.8 %. Thus, the radiator can be mounted directly on the roof and thermally insulated from below.

In the daytime, even a radiant surface without a selective coating, if it was not exposed to sunlight, removed heat in the form of radiation. The maximum possible amount of heat removed by radiation can be estimated in this case using the standard method for calculating heat transfer between two parallel plates. In this case, the temperature of the first plate was equal to the temperature of the condensation of the refrigerant, and the temperature of the second plate was equal to the temperature of the atmospheric air. The calculation under these conditions is presented in scenario 3.

Table 2

Parameters to consider for different heat transfer scenarios

Scenario	Parameters taken into account			Explanation
	Convection		Radiation	
	above	below		
0	Yes	Yes	No	at any time of the day, no thermal insulation from below, no heat exchange by radiation
1	Yes	No	According to the formula (2)	night, there is thermal insulation from below, ordinary color of the radiating surface
2	Yes	Yes	According to the formula (2)	night, no thermal insulation from below, ordinary color of the radiating surface
3	Yes	Yes	According to the Stefan-Boltzmann law	day, no thermal insulation from below, ordinary color of the radiating surface
4	Yes	No	According to the formula from [19]	day, there is thermal insulation from below, selective coating
5	Yes	Yes	According to the formula from [19]	day, no thermal insulation from below, selective coating

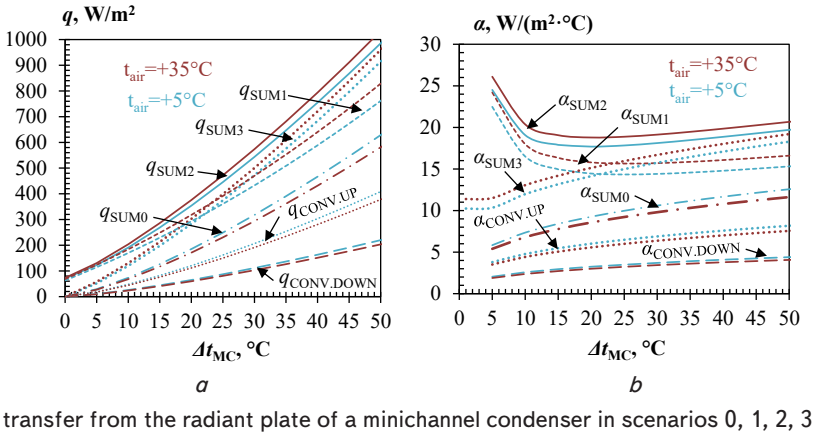

Fig. 6. Heat transfer from the radiant plate of a minichannel condenser in scenarios 0, 1, 2, 3 depending on the temperature difference Δt_{MC}: *a* – heat flux; *b* – total heat transfer coefficient

As can be seen from Fig. 6, *a*, at the same temperature difference under the combined action of radiation and convection, the radiating plate removed a greater amount of heat with an increase in the temperature of atmospheric air in scenarios 1, 2, and 3. Nevertheless, the effect of air temperature is small, and for practical purposes, it is possible to neglect change in ambient air temperature and take into account only the temperature difference on the condenser.

The total heat transfer coefficient due to convective and radiative heat transfer, calculated according to (6), is shown in Fig. 6, *b*. With a temperature difference from 10 to 50 °C in Scenario 1, the total heat transfer coefficient at night changed insignificantly and averaged $\alpha_{SUM1}=15.6$ W(m^2·°C). The use of the lower side of the radiating plate in scenario 2 made it possible to increase the heat transfer coefficient to $\alpha_{SUM2}=19.0$ W(m^2·°C).When using only convective heat exchange in scenario 0 from the upper and lower sides of the radiant plate $\alpha_{SUM0}=8.5$ W/(m^2·°C).

Similar calculations were carried out for daytime conditions using a coating of the radiating surface with a selective emission/absorption spectrum (scenarios 4 and 5).

With a temperature difference Δt_{MC} of 15 °C and an atmospheric air temperature of +5 °C, $q_{SUM4}=142.2$ W/m^2 was discharged from the radiating surface of the MC with a selective coating in the daytime, and at an atmospheric air temperature of +35 °C $q_{SUM1}=190.7$ W/m^2 (i.e. 34 % more).

The total heat transfer coefficient due to convective and radiative heat transfer, calculated according to (6), is shown in Fig. 7, *b*. In the specified range of atmospheric air temperatures and at a temperature difference of 15 °C, the heat transfer coefficient averaged $q_{SUM4}=11.0$ W/(m^2·°C). When using the lower surface for heat removal, the heat transfer coefficient increases on average to $q_{SUM5}=14.5$ W/(m^2·°C).

Table 3 shows the values of heat transfer coefficients for various considered MC application scenarios.

For MC without selective heat transfer coating and on the top and bottom side of the radiant plate, the heat transfer coefficient had a value in the range between scenario 0 and scenario 3 calculation. For a more accurate calculation, it is necessary to take into account scattered sunlight, which is beyond the scope of this study.

5. 1. 2. Permissible temperature change along the length of the radiating surface of the minichannel capacitor

Based on (13), the allowable change in the temperature of the MC radiating surface is calculated. Let the amount of heat removed from the radiating surface of a given MC be at least 95 % of the amount of heat removed from the surface of an MC with the same temperature at all points. The average temperature difference on the radiating surface between the condensing refrigerant and atmospheric air $\overline{\Delta t}_{MC.N}$ for an ordinary refrigeration machine should be 15 °C. Then $\Delta t_{PL}=1.5$ °C.

5. 1. 3. Required radiant plate thickness

The MC radiating plate is made of aluminium. The calculation of the thickness of the radiating plate according to (15) at $q_{SUM}=250$ W/m^2 and $\Delta t_{PL}=1.5$ °C showed that a decrease in the annular distance from 0.1 m to 0.05 m led to a decrease in the thickness of the radiating plate from 2 mm to 0.5 mm.

5. 1. 4. Material consumption and cost of a minichannel capacitor

The result of calculating the mass of 1 m^2 of the radiating surface, as well as the estimated cost of the materials used, are shown in Fig. 8. When calculating, it was taken into account that the capillary tubes have an inner diameter of at least 0.65 mm.

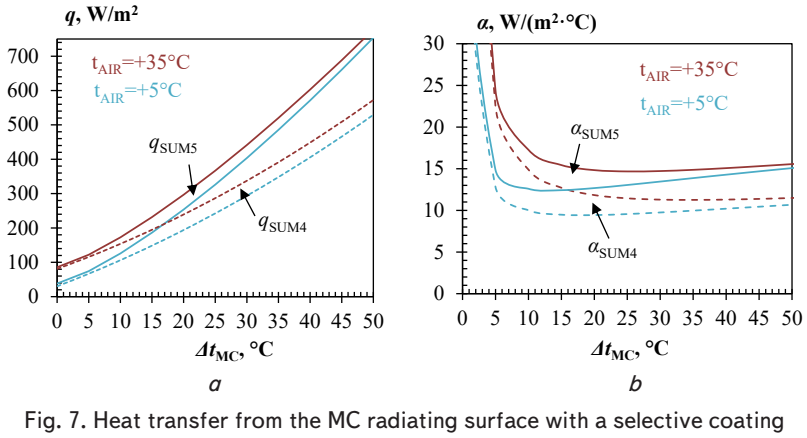

Fig. 7. Heat transfer from the MC radiating surface with a selective coating in scenarios 4 and 5 depending on the temperature difference MC: *a* — heat flux; *b* — the total heat transfer coefficient from the radiating surface

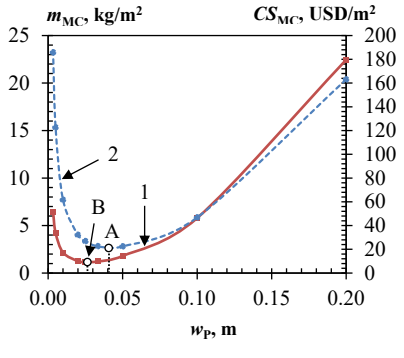

Fig. 8. MC characteristics depending on the distance between the tubes: 1 — mass of 1 m^2 of the radiating surface; 2 — estimated cost of materials

Taking the pitch between the tubes equal to 0.04 m, let's obtain the main parameters of the minichannel condenser (Table 4).

Table 3

Total heat transfer coefficient of the radiating plate at $\Delta t_{MC}=15$ °C, W/(m^2·°C)

Coating	Number of used radiant plate surfaces	Night	Day	
Without selective coating	1 (lower only)	15.6 (scenario 1)	min 6.0	max 10.2
	2 (lower and upper)	19.0 (scenario 2)	min 8.5 (scenario 0)	max 14.2 (scenario 3)
With selective coating	1 (lower only)	11.0 (scenario 4)	11.0 (scenario 4)	
	2 (lower and upper)	14.5 (scenario 5)	14.5 (scenario 5)	

Table 4

The main parameters of the minichannel condenser

Parameter		Designation	Unit	Value
Tube pitch		w_p	m	0.04
Inner diameter of capillary tube		$d_{P.IN}$	mm	0.65
Outer diameter of capillary tube		$d_{P.OUT}$	mm	1.9
Radiating plate thickness		Δ_{PL}	mm	0.32
Heat transfer coefficient from refrigerant		α_R	$W \cdot m^{-2} \cdot °C^{-1}$	16275
Coverage angle of the radiating surface		γ	°	27
Refrigerant mass per 1 m^2 of radiating surface at t_c=+45 °C according to formula (27)	R134a	$m_{R.f}$	kg/m^2	0.035
	R404a			0.032
	R410a			0.032
Mass of 1 m^2 of radiating surface according to (24)		–	kg/m^2	1.38

5. 1. 5. Angle of coverage of the radiating surface

Fig. 9 shows the result of calculating the angle of coverage of the radiating surface of the capillary tube according to (16).

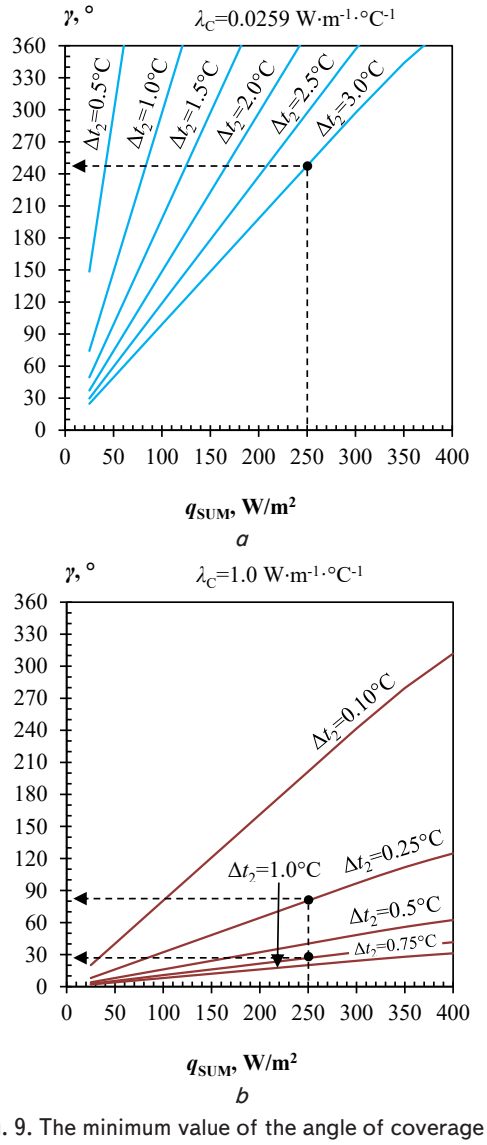

Fig. 9. The minimum value of the angle of coverage of the radiating surface depending on the heat flux removed from 1 m^2 of the MC radiating surface at different values of the allowable temperature change Δt_2: *a* – when the gap is filled with air; *b* – when the gap is filled with thermal paste KPT-8

If the gap is filled with air, it creates a large thermal resistance. Because of this, for transmission of 250 W/m^2, the angle of coverage must be 240° even at Δt_2=3.0 °C. When using thermal paste, the wrap angle can be 25° with a temperature change of 0.75 °C.

5. 1. 6. Theoretical heat transfer coefficient of the minichannel condenser

The MC heat transfer coefficient k_{MC} was calculated using (18), (17) based on the data in Tables 3, 4. The calculation results are presented in Table 5.

Table 5

Theoretical heat transfer coefficient MC ($W \cdot m^{-2} \cdot °C^{-1}$)

Coating	Number of used radiant plate surfaces	Night	Day	
without selective coating	1 (lower only)	14.6	min 5.9[1]	max 9.8
	2 (lower and upper)	17.6[2]	min 8.2[1]	max 13.4
with selective coating	1 (lower only)	10.5	10.5	
	2 (lower and upper)	13.7	13.7	

Note: 1 – in the absence of radiative heat transfer and wind; 2 – low air humidity and no clouds

Thus, the heat transfer coefficient, taking into account radiative cooling in the daytime, had a heat transfer coefficient from 9.8 to 13.7 $W \cdot m^{-2} \cdot °C^{-1}$. At night, theoretically, it increased to 17.6 $W \cdot m^{-2} \cdot °C^{-1}$. The values obtained are valid at air temperatures from +5 to +35 °C, in the absence of precipitation and wind, and the temperature difference Δt_{MC} is more than 10 °C.

5. 2. Experimental studies of the heat transfer coefficient of a minichannel condenser

In November 2022, a series of experimental studies were carried out aimed at determining the heat transfer coefficient of the minichannel condenser design. The experiments were carried out in the daytime and at night under various weather conditions (Tables 6–9).

The TEH supply voltage was not regulated. However, due to the increase in the city power supply voltage from 230 to 240 V, the TEH supply voltage increased from 93 to 97 V at night.

During the daytime, the heat transfer coefficient MC varied from 11.0±1.5 to 13.7±1.8 $W \cdot m^{-2} \cdot °C^{-1}$ depending on the environmental conditions without taking into account experiments when it was raining.

Table 6

Average temperatures in the experimental stand in the daytime

No.	Date	Time	Temperature, °C									
			t_0	t_C	t_1	t_2	t_{2S}	t_{3S}	t_3	t_{IN}	t_{OUT}	t_L
1	07.11	12:00–13:00	–22.1	24.6	–14.8	49.5	39.1	20.4	21.4	23.5	8.3	20.0
2	07.11	13:00–14:00	–20.3	24.9	–12.6	57	28.9	21.6	22.1	22.5	9.3	32.1
3	08.11	13:00–14:00	–20.3	19.7	–14.5	52.4	41.2	18.7	20.2	23.4	5.8	21.4
4	08.11	14:00–15:00	–20.3	20.3	–12.8	55.3	28.4	17.4	19.2	22.6	5.1	30.8
5	09.11	11:00–12:00	–22.2	24.4	–14.1	50.4	40.1	20.0	21.4	23.0	3.9	19.1
6	09.11	13:00–14:00	–20.3	23.9	–12.7	54.0	25.8	19.7	20.7	20.9	3.8	26.7
7	10.11	12:00–13:00	–22.1	22.3	–15.7	44.4	35.7	18.6	19.2	21.2	3.9	19.6
8	10.11	13:00–14:00	–20.3	21.7	–12.8	52.8	25.5	18.1	18.9	19.9	4.9	27.0
9	14.11	10:00–11:00	–20.3	24.2	–15.0	45.7	36.9	20.0	20.5	22.2	6.6	17.0
10	14.11	11:00–12:00	–20.3	23.8	–13.4	53.5	27.1	19.4	20.5	22.3	7.7	31.9

Table 7

Average values of the parameters in the experimental stand in the daytime at supply voltage U_{TEH}=93 V and TEH power Q_{TEH}=350 W

No.	Cloudiness CL, %	Precipitation	Pump	Q_0, W	Q_{MC}, W	Δt_{MC}, °C	k_{MC}, W·m^{-2}·°C^{-1}
1	0	no	off	364.4	447.8	16.3	13.7
2	0	no	on	363.6	418.3	15.5	13.5
3	100	rain	off	364.7	452.8	13.9	16.3
4	100	rain	on	364.0	424.8	15.2	14.1
5	100	no (snow on MC)	off	364.1	449.2	20.5	11.0
6	100	no (snow on MC)	on	363.2	412.7	20.0	10.3
7	0	no	off	363.9	424.8	18.4	12.0
8	0	no	on	362.9	413.2	16.9	12.3
9	0	no	off	363.6	441.3	17.7	12.5
10	0	no	on	363.6	417.5	16.2	12.9

Table 8

Average temperatures in the experimental stand at night

No.	Date	Time	Temperature, °C									
			t_0	t_C	t_1	t_2	t_{2S}	t_{3S}	t_3	t_{IN}	t_{OUT}	t_L
1	10.11	22:00–23:00	–22,1	19.9	–11.7	45.5	25.1	17.8	18.1	19.0	0.9	28.6
2	11.11	4:00–5:00	–23.1	18.8	–13.1	46.4	26.0	17.0	17.6	19.2	–1.4	30.1
3	14.11	22:00–23:00	–22.1	24.7	–13.1	47.8	38.6	19.9	21.1	23.6	5.7	18.0
4	15.11	4:00–5:00	–22.1	24.2	–13.1	48.3	39.1	20.2	21.2	23.6	2.4	18.0
5	15.11	22.00–23.00	–22.2	19.8	–13.1	46.3	37.3	17.2	17.8	22.7	3.1	18.4
6	16.11	4:00–5:00	–24.0	14.5	–13.2	44.6	35.9	13.5	15.1	22.3	1.7	17.9
7	21.11	22:00–23:00	–20.9	21.4	–13.0	47.6	38.5	18.2	19.5	23.7	6.1	18.9
8	22.11	4:00–5:00	–18.6	27.9	–12.4	49.6	40.3	22.1	23.1	23.7	8.2	18.9
9	22.11	22:00–23:00	–22.1	19.9	–14.3	46.7	38.0	17.2	18.4	23.8	5.0	19.1
10	23.11	22:00–23:00	–21.1	17.5	–13.4	46.4	37.4	15.5	16.5	23.2	3.3	18.8
11	23.11	22:00–23:00	–22.4	19.4	–15.6	46.0	36.7	17.4	17.9	23.0	3.9	18.3
12	24.11	22:00–23:00	–20.5	21.0	–11.6	47.2	38.1	18.4	19.3	23.6	1.9	18.5

Table 9

Average values of parameters in the experimental stand at night at supply voltage U_{TEH}=97 V and THE power Q_{TEH}=382 W

No.	Cloudiness CL, %	Precipitation	Pump	Q_0, W	Q_{MC}, W	Δt_{MC}, °C	k_{MC}, W·m^{-2}·°C^{-1}
1	0	no	on	395.2	445.8	19.0	11.7
2	0	no	on	395.5	452.5	20.1	11.2
3	100	no	off	396.6	482.0	19.0	12.7
4	75	no	off	396.6	483.2	21.9	11.1
5	100	no	off	396.4	479.0	16.7	14.3
6	100	rain	off	396.8	478.9	12.8	18.7
7	100	rain	off	396.3	484.0	15.4	15.8
8	100	no	off	395.3	482.5	19.8	12.3
9	100	rain	off	396.7	485.8	14.9	16.3
10	100	rain	off	396.2	482.4	14.1	17.1
11	100	rain	off	396.5	483.6	15.6	15.6
12	100	fog	off	396.1	479.5	19.0	12.6

The minimum daytime heat transfer coefficient values were obtained in experiments 5 and 6 when the MC was covered with snow. The maximum values of the heat transfer coefficient were obtained in experiments 3 and 4 when it was raining. At night, excluding periods when it was raining, the MC heat transfer coefficient varied from 11.1±1.5 to 12.7±1.7 $W \cdot m^{-2} \cdot °C^{-1}$.

Comparison of the results of experiments with the pump P on and off showed the following. When the pump was switched on, the temperature of the refrigerant vapor entering the MC decreased to 25...28 °C. The MC heat transfer coefficient decreased by no more than 15.6 % when the MC was covered with snow. In other cases, the decrease in the heat transfer coefficient did not exceed 6.8 %. Thus, it can be assumed that the actual steam temperature at the MC inlet can be neglected when calculating the heat transfer coefficient.

On the afternoon of November 17, 2022, an experiment was conducted to determine the possibility of snow thawing from the surface of the MC. It was snowing in the morning on that date. The experimental stand was turned off. As a result, a layer of snow 6 cm thick accumulated on the surface of the minichannel condenser (Fig. 10).

It took about 3.5 hours of compressor work to remove all the snow. The uniformity of snow melting across the width of the radiator confirmed that the refrigerant was evenly distributed over all capillary tubes.

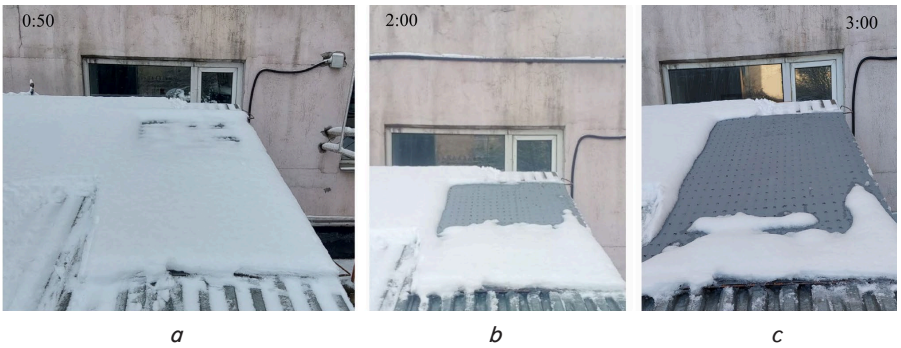

a *b* *c*

Fig. 10. Mini-channel condenser defrost (time since start of defrost in hh:mm format)

5. 3. Comparison of characteristics of mini-channel condenser and air-cooled condensers

The characteristics of conventional air-cooled condensers (ACC) of finned tube design were considered using the example of Guentner GCHC heat exchangers (Germany). The ACC technical characteristics are obtained from the GPC EU 2020 program (version 2020.19-225 c).

If the temperature difference on the condenser (the difference between the condensing temperature and the ambient air temperature) is 15 °C, at an ambient air temperature in the range of +20...+30 °C:

– the ACC average heat transfer coefficient (calculated on the basis of the temperature difference between the condensation temperature and the atmospheric air temperature) – 16.0...20.4 $W/(m^2 \cdot °C)$;

– thermal power transferred due to the consumption of 1 W of electric power by the fans: 54.0...104.4 W/W.

By dividing the ACC total mass (taking into account the mass of the heat exchanger, electric motors, fans, housing) by the area of its A_{ACC} heat exchange surface, let's obtain the specific mass of 1 m^2 of the heat exchange surface. For ACC, the specific gravity m_{ACC} was 0.95...1.77 kg/m^2.

For ACC, 0.044...0.047 kg of refrigerant is required per 1 m^2 of heat exchange surface.

Further, the ACC characteristics of a mini-channel design are determined using the Danfoss MCHE D1000-C heat exchanger as an example and information from [16]:

– average heat transfer coefficient – 25...60 $W/(m^2 \cdot °C)$;

– thermal power transferred due to consumption of 1 W electric power by fans: 33...68 W/W;

– weight of 1 m^2 of heat exchange surface 0.63...1.3 kg/m^2.

Comparison of MC with finned-tube ACC with forced air circulation showed the following (Table 10). At a temperature difference of 15 °C, no less than 210 W of heat was removed from 1 m^2 of the MC radiating surface under the experimental conditions. Under the same conditions, 255.0 W was removed from 1 m^2 of the heat exchange surface of the finned-tube ACC.

Thus, to replace 1 m^2 of the heat exchange surface of a finned-tube ACC during round-the-clock operation, 1.21 m^2 of the MC radiating surface is required. The MC mass will be 1.58 kg. The mass of a finned-tube ACC with forced air circulation with a similar output power is 0.95...1.77 kg. Thus, in some cases, when replacing rib-tube ACCs with MCs, the material consumption will not increase. This estimate does not include the mass of structures on which the MC will be attached.

The mass of ordinary microchannel air-cooled condensers is 4 times less than that of MC.

The amount of refrigerant charged to the MC radiator was about the same as the amount of refrigerant charged to the finned tube ACC.

The proposed MC design is extremely close in its characteristics to the design of air-cooled condensers with natural air circulation. The total heat transfer coefficients obtained in this study from the surface of a minichannel condenser are consistent with the data for air-cooled condensers [26]. The total heat transfer coefficient MC of the proposed design in the limiting case at night could theoretically reach 17.6 $W \cdot m^{-2} \cdot °C^{-1}$ at a temperature difference of 15 °C.

Table 10

Comparison of MC and ACC with forced air circulation

Heat exchanger	Minichannel condenser RC	Finned-tube ACC with forced air circulation	Microchannel condenser with forced air circulation
Removable thermal power, W	1000	1000	1000
Heat exchange surface area, m^2	4.76	3.84	–
Weight, kg	6.6	3.6...6.8	0.5...1.5
Power consumption, W	0	9.6...18.5	14...30

However, for traditional condensers with natural air circulation that do not use night radiative cooling, the heat transfer coefficient in [27] is stated at the level of 18.7 $W \cdot m^{-2} \cdot °C^{-1}$ at a temperature difference on the condenser of about 25 °C. Thus, the heat transfer coefficient MC is comparable to the ACC heat transfer coefficient with natural air circulation. At the same time, such a high heat transfer coefficient for ACC was apparently achieved due to an increase in the temperature difference. The MC design proposed in this paper theoretically makes it possible to obtain a comparable heat transfer coefficient at night at temperature differences of no more than 10–15 °C (see the SUM2 curve in Fig. 6, *b*).

6. Discussion of the results of the study of a minichannel capacitor

The obtained experimental data on the heat transfer coefficients MC are consistent with the results of theoretical calculations. At the same time, during the daytime, the experimental heat transfer coefficient (12.9±1.7 $W \cdot m^{-2} \cdot °C^{-1}$) approaches the maximum possible theoretical value (13.4 $W \cdot m^{-2} \cdot °C^{-1}$).

At night, the experimental heat transfer coefficient was practically the same as in the daytime. Those. no increase in the heat flux due to radiative cooling was observed in the experiments. Apparently, this is due to the fact that in the cold season, the removal of heat in the form of infrared radiation is hindered by fog, smog and high cloudiness.

The increase in thermal power transferred to the MC at night due to the increase in the power supply voltage has led to an increase in temperature difference. However, this did not cause a measurable increase in the heat transfer coefficient, which is consistent with the behavior of the heat transfer coefficient α_{SUM1} in Fig. 6, *b*.

On nights with high cloudiness, the heat transfer coefficient MC was about 12.0 $W \cdot m^{-2} \cdot °C^{-1}$. At the same time, according to the theory, the heat transfer coefficient could reach 14.3 $W \cdot m^{-2} \cdot °C^{-1}$ (approximately 19 % higher). This discrepancy can be explained by the imperfection of the MC manufacturing technology, due to which the capillary tubes did not always form a sufficiently tight contact with the radiating plate.

The paper [13] presents data on heat removal due to convection and radiative cooling from a radiating plate, the heat to which is supplied by a heat tube. This design diverted at night from 125 to 250 W/m^2 at a temperature difference of 10 to 18 °C and an ambient air temperature of about +4 °C. The heat transfer coefficient related to the area of the radiating surface was 12.5...13.8 W/m^2. Thus, the minichannel condenser proposed in this study removed a comparable amount of heat (222...242 W/m^2). The obtained values are apparently limited by the parameters of heat transfer from the radiating surface and in this case do not depend on the method of circulation of the refrigerant.

With a temperature difference in the MC at the level of 15 °C, the heat flux through the radiating surface of the MC was significantly greater than the heat flux of the radiator filled with coolant. Thus, in the review [28] it is shown that traditional liquid-cooled radiators remove only 30...85 W/m^2. In [29], a radiator with a selective coating removed 125±10 W/m^2 at night. The direct refrigerant supply can increase the heat flux by at least 1.7 times even when using only the upper side of the radiant plate without a selective coating.

The investigated MC produced cooling both during the day and at night. According to Table 7, in experiment 5, snow caused a decrease in the heat transfer coefficient by 25 % compared to experiments 7 and 9. Rain in experiment 3 increased the heat transfer coefficient by 20 %. Thus, the proposed scheme can be considered resistant to the influence of adverse environmental conditions.

It has been experimentally shown that snow could be removed from the radiating surface only due to the heat supplied by the coolant. The use of a thin radiating plate and small diameter refrigerant channels has made the MC structure easily deformed. Therefore, it is possible to cover various curved surfaces with them. The construction, made of small diameter copper tubes, withstands relatively high pressures. Accordingly, the MC can be charged with refrigerants such as R290, R410a, R32a or even R744.

The proposed MC design has a relatively high flow resistance to refrigerant flow and is not intended for use in natural circulation refrigeration systems.

Unlike traditional air conditioners, the proposed design of MC requires a large free area, which makes it impossible to use them if there are restrictions on the space occupied by the refrigeration system.

Experiments have shown that MC, protected from direct sunlight, can produce cooling both during the day and at night, even if its surface does not have a selective coating. Accordingly, the use of a selective coating of the radiating surface in this case is not a mandatory condition. However, MC with a selective coating does not require protection from direct sunlight.

MC can be used in stationary chillers where the condensing heat dissipated does not exceed a few kW. For example, they can be used in data center refrigeration systems, supermarket refrigeration, or chillers for small cold rooms, or small air conditioning systems (rooftops).

The theoretical calculation of the heat transfer coefficient did not take into account the effect of wind speed. The experimentally studied MC had a coating with uncertain optical properties. They should be explored in more detail in the future.

In this work, the infrared radiation flux was not measured. For a better understanding of the factors affecting the heat transfer of the radiating surface in winter, additional experimental studies using a pergeometer should be carried out. It is also possible to study the work of the MC in the summer. After that, the energy efficiency of the operation of refrigeration machines using the proposed minichannel condenser should be investigated.

7. Conclusions

1. Techniques have been developed to calculate the design parameters of the MC and its heat transfer coefficient. Calculations have shown that the thickness of the radiating aluminum plate can be reduced to 0.3 mm by reducing the distance between the tubes to 40 mm. At the same time, the mass of MC is reduced to 1.38 kg/m^2.

2. The conducted experiments showed that the heat transfer coefficient of a mini-channel condenser in winter at an air temperature of –2 to +9 °C changed from 10.0±1.3 to 18.7±2.5 $W \cdot m^{-2} \cdot °C^{-1}$ depending on the time of day and environmental conditions at a temperature difference from 12 to 20 °C. The heat flux was not less than 210±7.2 W/m^2. It exceeds at least 1.7 times the heat flow in the radiator for cooling the liquid coolant. The proposed MC design remained operational at high humidity, high cloudiness, in the presence of precipitation in the form of rain and snow. At night, there was no significant increase in the heat flux due to radiative cooling.

This is mainly due to the fact that during the considered period of the year, weather conditions (namely, a constant high level of cloudiness, fog and smog) prevented radiative cooling. Also, the proposed design is operable in the daytime, even in the absence of a selective coating of the radiating surface.

3. The area of the MC radiating surface should be 21 % larger than the area of the heat exchange surface of the finned-tube design with forced air circulation. The use of MC completely eliminates the consumption of electricity to remove the heat of condensation.

Conflict of interest

The authors declare that they have no conflict of interest in relation to this research, whether financial, personal, authorship or otherwise, that could affect the research and its results presented in this paper.

Financing

This study was funded by the Science Committee of the Ministry of Science and Higher Education of the Republic of Kazakhstan (Grant No. AP09258901).

Data availability

Experimental data are available upon request.

Acknowledgment

The authors of the work express their gratitude to the students of the Almaty Technological University (Republic of Kazakhstan) A. Minaev, M. Aleshchenko, T. Asylkhanov for assistance in mounting the experimental stand.

References

1. Dobson, R. (2005). Thermal modelling of a night sky radiation cooling system. Journal of Energy in Southern Africa, 16 (2), 20–31. doi: https://doi.org/10.17159/2413-3051/2005/v16i2a3184
2. Meir, M. G., Rekstad, J. B., LØvvik, O. M. (2002). A study of a polymer-based radiative cooling system. Solar Energy, 73 (6), 403–417. doi: https://doi.org/10.1016/s0038-092x(03)00019-7
3. Anderson, T., Duke, M., Carson, J. (2013). Performance of an unglazed solar collector for radiant cooling. Australian Solar Cooling 2013 Conference. Available at: https://openrepository.aut.ac.nz/handle/10292/5651?show=full
4. Vidhi, R. (2018). A Review of Underground Soil and Night Sky as Passive Heat Sink: Design Configurations and Models. Energies, 11 (11), 2941. doi: https://doi.org/10.3390/en11112941
5. Bagiorgas, H. S., Mihalakakou, G. (2008). Experimental and theoretical investigation of a nocturnal radiator for space cooling. Renewable Energy, 33 (6), 1220–1227. doi: https://doi.org/10.1016/j.renene.2007.04.015
6. Hollick, J. (2012). Nocturnal Radiation Cooling Tests. Energy Procedia, 30, 930–936. doi: https://doi.org/10.1016/j.egypro.2012.11.105
7. Tsoy, A. P., Baranenko, A. V., Granovsky, A. S., Tsoy, D. A., Dzhamasheva, R. A. (2020). Energy efficiency analysis of a combined cooling system with night radiative cooling. AIP Conference Proceedings. doi: https://doi.org/10.1063/5.0026908
8. Karagusov, V. I., Serdyuk, V. S., Kolpakov, I. S., Nemykin, V. A., Pogulyaev, I. N. (2018). Experimental determination of rate and direction of heat flow of the radiation life – Support system with vacuum heat insulation. AIP Conference Proceedings. doi: https://doi.org/10.1063/1.5051876
9. Goldstein, E. A., Raman, A. P., Fan, S. (2017). Sub-ambient non-evaporative fluid cooling with the sky. Nature Energy, 2 (9). doi: https://doi.org/10.1038/nenergy.2017.143
10. Goldstein, E. A., Nasuta, D., Li, S., Martin, C., Raman, A. (2018). Free Subcooling with the Sky: Improving the efficiency of air conditioning systems. 17th International Refrigeration and Air Conditioning Conference at Purdue. Available at: https://docs.lib.purdue.edu/iracc/1913/
11. Tsoy, A., Granovskiy, A., Tsoy, D., Koretskiy, D. (2022). Cooling capacity of experimental system with natural refrigerant circulation and condenser radiative cooling. Eastern-European Journal of Enterprise Technologies, 2 (8 (116)), 45–53. doi: https://doi.org/10.15587/1729-4061.2022.253651
12. Ezekwe, C. I. (1990). Performance of a heat pipe assisted night sky radiative cooler. Energy Conversion and Management, 30 (4), 403–408. doi: https://doi.org/10.1016/0196-8904(90)90041-v
13. Yu, C., Shen, D., Jiang, Q., He, W., Yu, H., Hu, Z. et al. (2019). Numerical and Experimental Study on the Heat Dissipation Performance of a Novel System. Energies, 13 (1), 106. doi: https://doi.org/10.3390/en13010106
14. Kim, M.-H., Lee, S. Y., Mehendale, S. S., Webb, R. L. (2003). Microchannel Heat Exchanger Design for Evaporator and Condenser Applications. Advances in Heat Transfer, 297–429. doi: https://doi.org/10.1016/s0065-2717(03)37004-2
15. Butrymowicz, D., Śmierciew, K., Gagan, J., Dudar, A., Łukaszuk, M., Zou, H., Łapiński, A. (2022). Investigations of Performance of Mini-Channel Condensers and Evaporators for Propane. Sustainability, 14 (21), 14249. doi: https://doi.org/10.3390/su142114249
16. Boeng, J., Rametta, R. S., Melo, C., Hermes, C. J. L. (2020). Thermal-hydraulic characterization and system-level optimization of microchannel condensers for household refrigeration applications. Thermal Science and Engineering Progress, 20, 100479. doi: https://doi.org/10.1016/j.tsep.2020.100479
17. Walton, G. (1983). Thermal Analysis Research Program. Washington, 292. Available at: https://ntrl.ntis.gov/NTRL/dashboard/searchResults/titleDetail/PB83194225.xhtml

18. Samuel, D. G. L., Nagendra, S. M. S., Maiya, M. P. (2013). Passive alternatives to mechanical air conditioning of building: A review. Building and Environment, 66, 54–64. doi: https://doi.org/10.1016/j.buildenv.2013.04.016
19. Zhao, D., Aili, A., Zhai, Y., Xu, S., Tan, G., Yin, X., Yang, R. (2019). Radiative sky cooling: Fundamental principles, materials, and applications. Applied Physics Reviews, 6 (2), 021306. doi: https://doi.org/10.1063/1.5087281
20. Zhao, D., Aili, A., Zhai, Y., Lu, J., Kidd, D., Tan, G. et al. (2019). Subambient Cooling of Water: Toward Real-World Applications of Daytime Radiative Cooling. Joule, 3 (1), 111–123. doi: https://doi.org/10.1016/j.joule.2018.10.006
21. Mukhachev, G. A., Schukin, V. K. (1991). Termodinamika i teploperedacha. Moscow: Vysshaya shkola.
22. Bohdal, T., Charun, H., Sikora, M. (2012). Heat transfer during condensation of refrigerants in tubular minichannels. Archives of Thermodynamics, 33 (2), 3–22. doi: https://doi.org/10.2478/v10173-012-0008-x
23. Isachenko, V. P., Osipova, V. A., Sukomel, A. (1975). Teploperedacha. Moscow: Energiya, 315.
24. Tevar, J. A. F., Castaño, S., Marijuán, A. G., Heras, M. R., Pistono, J. (2015). Modelling and experimental analysis of three radioconvective panels for night cooling. Energy and Buildings, 107, 37–48. doi: https://doi.org/10.1016/j.enbuild.2015.07.027
25. Bell, I. H., Wronski, J., Quoilin, S., Lemort, V. (2014). Pure and Pseudo-pure Fluid Thermophysical Property Evaluation and the Open-Source Thermophysical Property Library CoolProp. Industrial & Engineering Chemistry Research, 53 (6), 2498–2508. doi: https://doi.org/10.1021/ie4033999
26. Orzechowski, T., Stokowiec, K. (2014). Free convection on a refrigerator's condenser. EPJ Web of Conferences, 67, 02089. doi: https://doi.org/10.1051/epjconf/20146702089
27. Saleh, A. A. M. (2019). Correlation of overall heat transfer coefficient in the three zones of wire and tube condenser. Journal of Mechanical Engineering Research and Developments, 42 (1), 96–103. doi: https://doi.org/10.26480/jmerd.01.2019.96.103
28. Ahmad, M. I., Jarimi, H., Riffat, S. (2019). Nocturnal Cooling Technology for Building Applications. Springer, 70. https://doi.org/10.1007/978-981-13-5835-7
29. Aili, A., Zhao, D., Lu, J., Zhai, Y., Yin, X., Tan, G., Yang, R. (2019). A kW-scale, 24-hour continuously operational, radiative sky cooling system: Experimental demonstration and predictive modeling. Energy Conversion and Management, 186, 586–596. doi: https://doi.org/10.1016/j.enconman.2019.03.006